

## Transmission electron microscopic observation of nanoindentations made on ductile-machined silicon wafers

|                              |   |
|------------------------------|---|
| 著者                           | 厨川 常元   |
| journal or publication title | Applied Physics Letters   |
| volume                       | 87  |
| number                       | 21  |
| page range                   | 211901-1-211901-3   |
| year                         | 2005  |
| URL                          | <a href="http://hdl.handle.net/10097/34914">http://hdl.handle.net/10097/34914</a> |

## Transmission electron microscopic observation of nanoindentations made on ductile-machined silicon wafers

Jiawang Yan<sup>a)</sup>

*Department of Nanomechanics, Tohoku University, Aramaki Aoba 6-6-01, Aoba-ku, Sendai, 980-8579, Japan*

Hirokazu Takahashi and Jun'ichi Tamaki

*Department of Mechanical Engineering, Kitami Institute of Technology, Koen-cho 165, Kitami, Hokkaido 090-8507, Japan*

Xiaohui Gai

*Department of Material Science and Engineering, Tohoku University, Aobayama-02, Aoba-ku, Sendai, 980-8579, Japan*

Tsunemoto Kuriyagawa

*Department of Nanomechanics, Tohoku University, Aramaki Aoba 6-6-01, Aoba-ku, Sendai, 980-8579, Japan*

(Received 8 August 2005; accepted 22 September 2005; published online 14 November 2005)

Nanoindentation tests were performed on a ductile-machined silicon wafer with a Berkovich diamond indenter, and the resulting indents were examined with a transmission electron microscope. It was found that the machining-induced subsurface amorphous layer undergoes significant plastic flow, and the microstructure of the indent depends on the indentation load. At a small load ( $\sim 20$  mN), most of the indented region remains to be amorphous with minor crystalline nuclei; while under a large load ( $\sim 50$  mN), the amorphous phase undergoes intensive recrystallization. The understanding and utilization of this phenomenon might be useful for improving the microscopic surface properties of silicon parts produced by a ductile machining process. © 2005 American Institute of Physics. [DOI: 10.1063/1.2133908]

Single-crystal silicon has a strong directional covalent bond with the diamond-cubic structure and is nominally a highly brittle material at room temperature. However, silicon can also be deformed and machined in a ductile manner under high-pressure conditions due to the high-pressure phase transformations.<sup>1–11</sup> This phenomenon has attracted intense interest from multidisciplinary researchers, and the thorough understanding of this phenomenon may contribute significantly to the technological developments of manufacturing industries for semiconductor substrates and microelectromechanical systems.<sup>12</sup>

Ductile regime machining using a single-crystal diamond tool at an extremely small depth scale, from a few nanometers to a few tens of nanometers, is a potential technology for fabricating silicon components of complex shapes.<sup>13</sup> This technology can produce ultraprecise silicon parts, but at the same time, may cause the near-surface layer of material to transform to an amorphous state via a metastable metallic ( $\beta$ -Sn) phase. A number of previous studies have confirmed the presence of the amorphous phase in ductile-machined silicon wafers.<sup>8–11</sup>

The residual amorphous layer will significantly influence the mechanical, optical, and electrical functions of silicon parts, as well as the subsequent wafer manufacturing processes.<sup>14</sup> Therefore, it is very important to clarify the nature of this amorphous layer. In a recent paper, we reported the preliminary results of nanoindentation tests performed on ductile-machined silicon wafers.<sup>15</sup> We found that the machining-induced amorphous layer is softer than the

diamond-cubic silicon and has significant microplasticity, which in fact determines the ductile machining performance of silicon substrates. In the present letter, we report the transmission electron microscopic observation results of the indents made on a ductile-machined silicon surface, and investigate the deformation and possible phase transformation behavior of the amorphous layer.

Electric device grade *p*-type single-crystal silicon (100) wafers were machined by fly-cutting using a  $-60^\circ$  rake angle diamond cutting tool on an ultraprecision diamond lathe, Toyoda AHP 20-25N. Undeformed chip thickness was set to 100 nm and cutting speed was 15–18 m/s. The nanoindentation tester we used was ENT-1100a, produced by Elionix Co., Ltd. (Tokyo, Japan). Tests were performed using a Berkovich-type diamond indenter. The maximum load was varied in the range of 0.1–100 mN, where the time for loading and unloading was the same and fixed at 5 s. Other conditions can be partially found in Ref. 15.

One of the diamond-machined silicon wafers with nanoindentations was processed by focused ion beam (FIB) technique to prepare transmission electron microscope (TEM) samples. The TEM we used was H-9000NAR, produced by Hitachi Ltd. (Tokyo, Japan). The conditions used for TEM observations were: Acceleration voltage 300 kV, direct magnification from 5000 to 400 000 times and extension magnification of five times, leading to a total magnification from 25 000 to 2 000 000 times. To protect from possible damages from the FIB, carbon (C) and tungsten (W) coatings were made on the samples.

Figure 1 shows a bright-field cross-sectional TEM (XTEM) micrograph of the ductile-machined silicon wafer near one of the indents. It can be seen that an approximately

<sup>a)</sup>Electronic mail: yanjw@pm.mech.tohoku.ac.jp

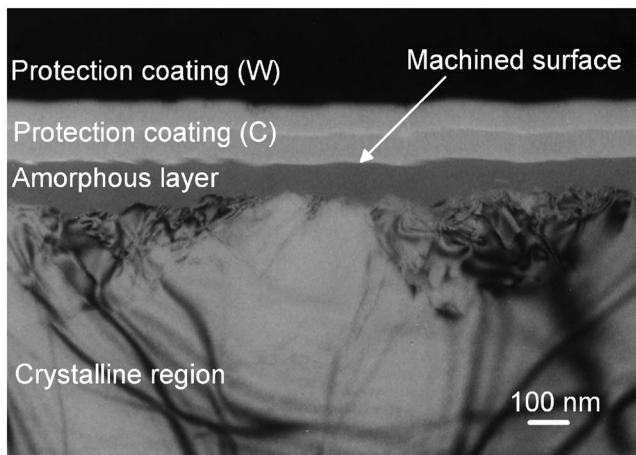


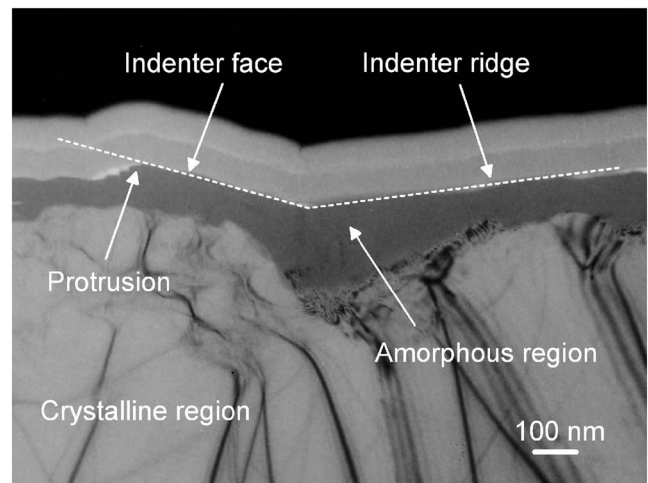
FIG. 1. Bright-field XTEM micrograph of a diamond-machined silicon wafer.

150-nm-thick phase transformation layer has been generated on the silicon substrate by machining, and high-resolution TEM (HRTEM) observation showed that this layer is completely amorphous. Below the amorphous layer, a few dislocations can be seen in the crystalline region. The long stripes shown at the bottom half of the photograph are interference fringes caused by the bending of the TEM sample due to FIB processing.

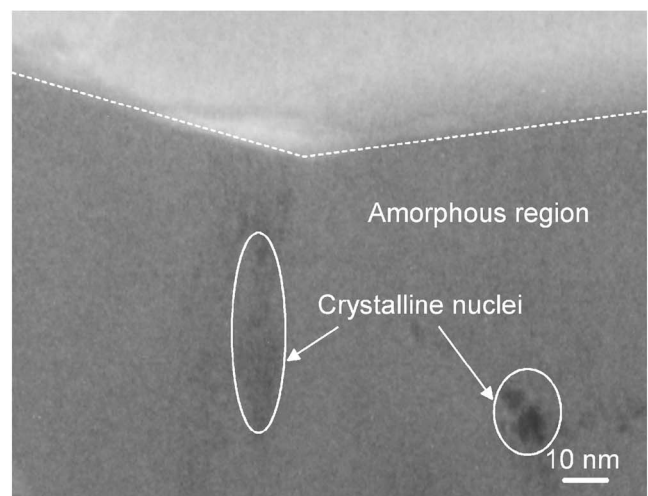
Figure 2(a) is an XTEM micrograph of an indent made at a maximum load of 20 mN. The amorphous layer right below the indenter tip becomes apparently thicker than the unindented regions, indicating that the existing amorphous layer has been penetrated by the indenter and a new amorphous zone was formed by the indentation. On the left side of the indent, which corresponds to one of the faces of the indenter, a protrusion about 100 nm higher than the original surface can be observed, which was caused by the side flow of the amorphous silicon. Figure 2(b) is an enlarged view of the region around the indenter tip. Most of the region is in a uniform amorphous state, while a few extremely small dark spots can be seen, which indicates the existence of crystalline nuclei.

Figure 3(a) is an XTEM micrograph of an indent made at a maximum load of 50 mN. It can be seen that in this case the phase transformation region due to indentation has become apparently larger than that shown in Fig. 2(a). Below the phase transformation region, a median crack is extending downward, which indicates that the critical load for microfracture initiation has been exceeded. What to be note here is that the appearance of the phase transformation region is distinctly different from that shown in Fig. 2(a). The microstructure of the material within this region exhibits significant heterogeneity, although the side protrusion and its adjacent surface region still remain to be uniform amorphous state. Figure 3(b) is an HRTEM micrograph of a small region under the indenter tip in Fig. 3(a). As indicated by dotted lines, numerous crystalline grains of nano- or ten-nano-level size are surrounded by the amorphous phase (*a*-Si). The nanocrystalline grains are irregular in shape and size, and the lattice orientations of these grains are different from one to another. By comparing the results in Figs. 2 and 3, it is considerable that under high load conditions, the machining-induced *a*-Si phase undergoes recrystallization, while the recrystallization is insignificant under small load conditions.

Downloaded 13 Jul 2008 to 130.34.135.158. Redistribution subject to AIP license or copyright; see <http://apl.aip.org/apl/copyright.jsp>



(a)



(b)

FIG. 2. XTEM micrographs of an indent made at a maximum load of 20 mN: (a) General view and (b) enlarged view of the region around the indenter tip.

The crystallization of *a*-Si is a noteworthy phenomenon and has been already confirmed in various laser irradiation processes.<sup>16–18</sup> The short-pulse lasers crystallize the *a*-Si via a rapid melting and solidification process, the resulting material structure depending on the irradiation energy of the lasers and the substrate properties of the specimen. The crystallization of *a*-Si due to high pressure has also been predicted in the total energy calculations.<sup>19</sup>

In contrast to the crystalline-amorphous phase transformations, the transformation from amorphous to crystalline phases during indentation tests of silicon is still an area of controversy. Knapp *et al.*<sup>20</sup> performed nanoindentations on self-ion-implanted *a*-Si but could not observe phase transformations. However, indentations with a Vickers indenter at a high load (137 mN) on self-ion-implanted *a*-Si did show phase transformation to Si-III (body-centered cubic).<sup>21</sup> The results from the present work indicated again the possibility of completely mechanically induced crystallization of *a*-Si, although we cannot reach definitive conclusions about the structure of the new crystalline phase based on the present results. Also, from the results of the present work, we may assume that the indentation load Knapp *et al.*<sup>20</sup> used might have been too small ( $\sim 5$  mN) to induce phase transformations.

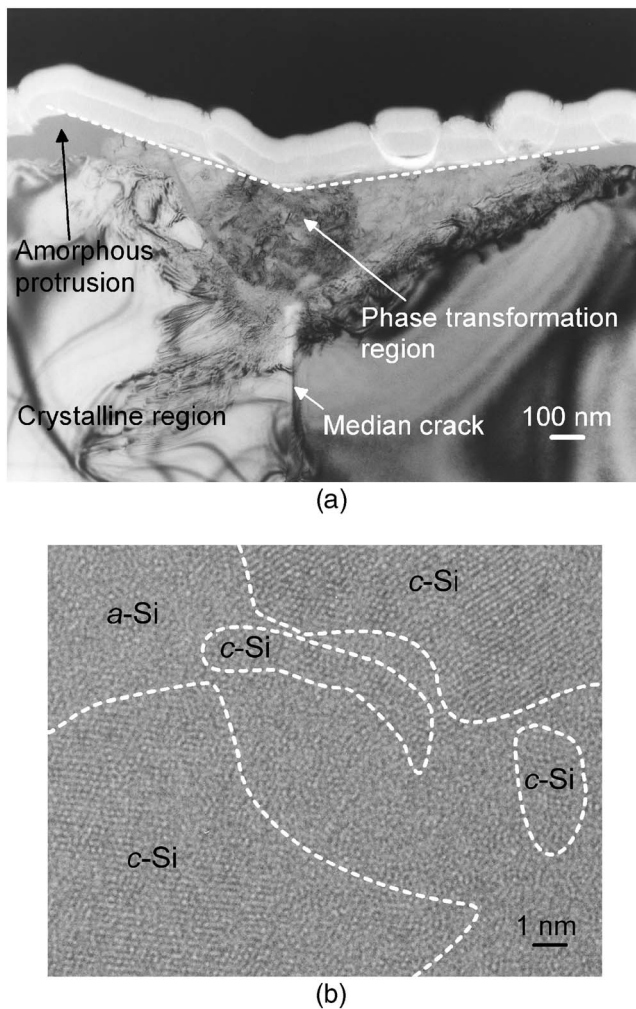


FIG. 3. XTEM micrographs of an indent made at a maximum load of 50 mN: (a) General view and (b) HRTEM of a small region below the indenter tip.

Apart from the indentation load, other conditions, such as loading/unloading rate and indenter geometry,<sup>22,23</sup> may also influence the residual microstructure of the amorphous layer. From this point of view, it might be possible to control the microstructure of the indented area through optimizing the indentation conditions. The above-mentioned mechanical process, that is, diamond turning followed by nanoindentation, might provide an alternative possibility for fabricating high-performance thin-film transistors and other useful

devices<sup>24–26</sup> instead of the laser-induced crystallization of *a*-Si. Similarly, in a ductile machining process, it might also be possible to control the microstructure of the near-surface layer of a silicon part by controlling the tool geometry and machining conditions.

- <sup>1</sup>I. V. Gridneva, Y. V. Milman, and V. I. Trefilov, *Phys. Status Solidi A* **14**, 177 (1972).
- <sup>2</sup>V. G. Eremenko and V. I. Nikitenko, *Phys. Status Solidi A* **14**, 317 (1972).
- <sup>3</sup>D. R. Clarke, M. C. Kroll, P. D. Kirchner, and R. F. Cook, *Phys. Rev. Lett.* **60**, 2156 (1988).
- <sup>4</sup>G. M. Pharr, W. C. Oliver, and D. S. Harding, *J. Mater. Res.* **6**, 1129 (1991).
- <sup>5</sup>D. L. Callahan and J. C. Morris, *J. Mater. Res.* **7**, 1614 (1992).
- <sup>6</sup>A. Kailer, Y. G. Gogotsi, and K. G. Nickel, *J. Appl. Phys.* **81**, 3057 (1997).
- <sup>7</sup>J. E. Bradby, J. S. Williams, J. Wong-Leung, M. V. Swain, and P. Munroe, *Appl. Phys. Lett.* **77**, 3749 (2000).
- <sup>8</sup>K. E. Puttick, L. C. Whitmore, C. L. Chao, and A. E. Gee, *Philos. Mag. A* **69**, 91 (1994).
- <sup>9</sup>T. Shibata, A. Ono, K. Kurihara, E. Makino, and M. Ikeda, *Appl. Phys. Lett.* **65**, 2553 (1994).
- <sup>10</sup>B. V. Tanikella, A. H. Somasekhar, A. T. Sowers, R. J. Nemanich, and R. O. Scattergood, *Appl. Phys. Lett.* **69**, 2870 (1996).
- <sup>11</sup>C. Jaynes, K. E. Puttick, L. C. Whitmore, K. Gartner, A. E. Gee, D. K. Millen, R. P. Webb, R. M. A. Peel, and B. J. Sealy, *Nucl. Instrum. Methods Phys. Res. B* **118**, 431 (1996).
- <sup>12</sup>J. Yan, M. Yoshino, T. Kuriyagawa, T. Shirakashi, K. Syoji, and R. Komanduri, *Mater. Sci. Eng., A* **297**, 230 (2001).
- <sup>13</sup>J. Yan, K. Syoji, T. Kuriyagawa, and H. Suzuki, *J. Mater. Process. Technol.* **121**, 363 (2002).
- <sup>14</sup>J. Yan, *J. Appl. Phys.* **95**, 2094 (2004).
- <sup>15</sup>J. Yan, H. Takahashi, J. Tamaki, X. Gai, H. Harada, and J. Patten, *Appl. Phys. Lett.* **86**, 181913 (2005).
- <sup>16</sup>Y. L. Khait, R. Beserman, A. Chack, R. Weil, and W. Beyer, *Appl. Phys. Lett.* **81**, 3347 (2002).
- <sup>17</sup>G. D. Ivlev and E. I. Gatskevich, *Semiconductors* **37**, 604 (2003).
- <sup>18</sup>T. Y. Choi, D. J. Hwang, and C. P. Grigoropoulos, *Opt. Eng. (Bellingham)* **42**, 3383 (2003).
- <sup>19</sup>M. Durandurdu and D. A. Drabold, *Phys. Rev. B* **67**, 212101 (2003).
- <sup>20</sup>J. A. Knapp, D. M. Follstaedt, S. M. Myers, and G. A. Petersen, *Mater. Res. Soc. Symp. Proc.* **649**, Q1.2.1 (2001).
- <sup>21</sup>M. M. Khayyat, G. K. Banini, D. G. Hasko, and M. M. Chaudhri, *J. Phys. D* **36**, 1300 (2003).
- <sup>22</sup>H. Saka, A. Shimatani, M. Suganuma, and Suprijadi, *Philos. Mag. A* **82**, 1971 (2002).
- <sup>23</sup>J. Jang, M. J. Lance, S. Wen, T. Y. Tsui, and G. M. Pharr, *Acta Mater.* **53**, 1759 (2005).
- <sup>24</sup>M. Ivanda, K. Furic, O. Gamulin, M. Persin, and D. Gracin, *J. Appl. Phys.* **70**, 4637 (1991).
- <sup>25</sup>R. Z. Bachrach, K. Winer, J. B. Boyce, S. E. Ready, R. I. Johnson, and G. B. Anderson, *J. Electron. Mater.* **19**, 241 (1990).
- <sup>26</sup>L. P. Avakyants, V. S. Gorelik, I. A. Kurova, and A. V. Chervyakov, *Solid State Phys.* **39**, 1925 (1997).